Development 127, 779-790 (2000)
Printed in Great Britain © The Company of Biologists Limited 2000
DEV7769

The *Fab-8* boundary defines the distal limit of the bithorax complex *iab-7* domain and insulates *iab-7* from initiation elements and a PRE in the adjacent *iab-8* domain

Stéphane Barges[1], Jozsef Mihaly[1,*], Mireille Galloni[1,‡], Kirsten Hagstrom[2,§], Martin Müller[1,2], Greg Shanower[2], Paul Schedl[2], Henrik Gyurkovics[3] and François Karch[1,¶]

[1]Department of Zoology and Animal Biology, University of Geneva, 30 quai E. Ansermet, CH-1211 Geneva 4, Switzerland
[2]Department of Molecular Biology, Princeton University, Princeton, NJ 08544, USA
[3]Institut of Genetics, Biological Research Center, Hungarian Academy, H-6701 Szeged, Hungary
*Present address: Developmental Biology program, EMBL, Meyerhofstr. 1, D-69117 Heidelberg, Germany
‡Present address: Fred Hutchinson Cancer Research Center, Seattle, Washington 98109, USA
§Present address: Department of Molecular and Cell Biology, University of California, Berkeley, CA 94720-3204, USA
¶Author for correspondence (e-mail: karch@sc2a.unige.ch)

Accepted 24 November 1999; published on WWW 26 January 2000

SUMMARY

The *Drosophila* bithorax complex *Abdominal-B* (*Abd-B*) gene specifies parasegmental identity at the posterior end of the fly. The specific pattern of *Abd-B* expression in each parasegment (PS) determines its identity and, in PS10-13, *Abd-B* expression is controlled by four parasegment-specific *cis*-regulatory domains, *iab-5* to *iab-8*, respectively. In order to properly determine parasegmental identity, these four *cis*-regulatory domains must function autonomously during both the initiation and maintenance phases of BX-C regulation. The studies reported here demonstrate that the (centromere) distal end of *iab-7* domain is delimited by the *Fab-8* boundary. Initiators that specify PS12 identity are located on the proximal *iab-7* side of *Fab-8*, while initiators that specify PS13 identity are located on the distal side of *Fab-8*, in *iab-8*. We use transgene assays to demonstrate that *Fab-8* has enhancer blocking activity and that it can insulate reporter constructs from the regulatory action of the *iab-7* and *iab-8* initiators. We also show that the *Fab-8* boundary defines the realm of action of a nearby *iab-8* Polycomb Response Element, preventing this element from ectopically silencing the adjacent domain. Finally, we demonstrate that the insulating activity of the *Fab-8* boundary in BX-C is absolutely essential for the proper specification of parasegmental identity by the *iab-7* and *iab-8 cis*-regulatory domains. *Fab-8* together with the previously identified *Fab-7* boundary delimit the first genetically defined higher order domain in a multicellular eukaryote.

Key words: Bithorax complex, Chromatin domain boundary, Insulator, *Polycomb* Response Element, *Drosophila*

INTRODUCTION

The three homeotic genes of the bithorax complex, *Ultrabithorax* (*Ubx*), *abdominal-A* (*abd-A*) and *Abdominal-B* (*Abd-B*) are responsible for specifying the identity of parasegments 5 to 14 (PS5-PS14), which form the posterior half of the thorax and all abdominal segments of the adult fly (Lewis, 1978; Sanchez-Herrero et al., 1985). The PS-specific expression patterns of *Ubx*, *abd-A* and *Abd-B* are generated by a complicated *cis*-regulatory region that spans a DNA segment of 300 kb. This *cis*-regulatory region is organized in a series of nine parasegment-specific domains, *abx/bx, bxd/pbx, iab-2* to *iab-8* (for reviews see Duncan, 1987; Peifer et al., 1987). Each domain directs expression of one of the BX-C homeotic genes in a specific parasegment. For example, *Abd-B* expression in PS10, PS11, PS12 and PS13 is controlled by the *iab-5*, *iab-6*, *iab-7* and *iab-8 cis*-regulatory domains, respectively (Celniker et al., 1990; Sanchez-Herrero, 1991). These *cis*-regulatory domains are located downstream of the *Abd-B* transcription unit (see Fig. 1) and, as is the case for the other BX-C *cis*-regulatory domains, their proximal-distal order along the chromosome corresponds to the anteroposterior order of the parasegments that they specify.

Regulation of the BX-C homeotic genes can be divided into two phases, initiation and maintenance. The choice of parasegment identity is made during the initiation phase, and depends upon the activity of the gap and pair-rule gene products that are present in the parasegment (Simon et al., 1990; Qian et al., 1991; Muller and Bienz, 1992). These proteins interact with initiation elements in each *cis*-regulatory domain, sequentially activating the domains in progressively more posterior parasegments. For example, the regulatory proteins present in PS12 activate *iab-7*, but not *iab-8*, while the proteins in PS13 activate *iab-8*. Because the products of the

gap and pair-rule genes are expressed only transiently in the early embryo, the activity state selected during the initiation phase is fixed by the programming of a maintenance system in each *cis*-regulatory domain. This maintenance system requires the *Polycomb-Group (Pc-G)* and *trithorax-Group (trx-G)*. The products of the *Pc-G* genes function as negative regulators, maintaining the inactive state of the homeotic genes, while the products of the *trx-G* function as positive regulators, maintaining the active state. *Pc-G*-mediated repression is thought to resemble mating type silencing in yeast and involve the formation of chromatin structures that are inaccessible to *trans*-acting regulators (McCall and Bender 1996; Boivin and Dura 1998; for reviews see Paro, 1990; Kennison and Tamkun, 1992; Simon, 1995; Pirrotta, 1997). The repressive *Pc-G* complexes are first assembled during the transition from the initiation phase to the maintenance phase (Poux et al., 1996) and exert their regulatory effects by interacting with specific elements in each *cis*-regulatory domain, called Polycomb Response Elements or PREs (Simon et al., 1990, 1993; Müller and Bienz, 1991; Chan et al., 1994; Chiang et al., 1995). The activity state of the PREs in each *cis*-regulatory domain appears to be programmed by the initiator elements; however, it is not yet clear whether this involves a direct interaction of gap and pair-rule gene products with components of the PRE or requires other intermediary factors.

Implicit in this model for the functional organization of the BX-C *cis*-regulatory domains is a mechanism(s) to ensure their autonomy. One possible mechanism has been suggested by the discovery of an unusual dominant mutation called *Fab-7*^{1}, which deletes a 4 kb DNA segment between the *iab-6* and *iab-7 cis*-regulatory domains (Gyurkovics et al., 1990). While most mutations in BX-C *cis*-regulatory domains have a loss-of-function phenotype, *Fab-7*^{1} is unusual in that it has a gain-of-function phenotype, transforming PS11 into a copy of PS12. This transformation arises from the inappropriate activation of the *iab-7 cis*-regulatory domain in PS11 where *iab-6* normally functions. As a consequence, *Abd-B* is expressed in a PS12-like pattern in PS11 (Galloni et al., 1993). The novel properties of *Fab-7*^{1} led to the hypothesis that the mutation deletes a chromatin domain boundary element that insulates the *iab-6 cis*-regulatory domain from *iab-7*; in the absence of this boundary, the two domains are no longer autonomous but instead fuse into a single *cis*-regulatory domain. Consequently, positive elements in *iab-6* ectopically activate *iab-7* in PS11 (for review, see Mihaly et al., 1998).

This hypothesis has been supported and refined by transgene assays for boundary function and by the analysis of additional deletions in *Fab-7*. Transgene assays have shown that the DNA segment deleted in the original *Fab-7*^{1} mutation actually contains two distinct elements. On the proximal side, there is a boundary element that spans two prominent chromatin-specific nuclease hypersensitive regions. In transgene assays, this element blocks enhancer:promoter interactions (Hagstrom et al., 1996; Zhou et al., 1996). On the distal side, there is a PRE for the *iab-7 cis*-regulatory domain which spans a single chromatin-specific nuclease hypersensitive region. In transgene assays, this element functions as a Pc-G-dependent silencer (Hagstrom et al., 1997). The conclusions drawn from transgene assays have been confirmed by the phenotypic properties of a series of BX-C deletions that remove just the boundary element or the PRE (Mihaly et al., 1997). Like the original *Fab-7*^{1} allele, boundary deletions cause a dominant transformation of PS11 into PS12. However, these deletions differ from *Fab-7*^{1} in that there are often small clones of cells in PS11 that exhibit a loss-of-function phenotype and assume PS10 identity. In these clones, *iab-6* is ectopically silenced in PS11, and, as a consequence, *Abd-B* expression is controlled by *iab-5*. The mixed gain- and loss-of-function phenotypes in the deletions that only remove the boundary arise because there is a competition in the fused *cis*-regulatory domain between positive elements in *iab-6* that ectopically activate *iab-7* and negative elements in *iab-7* that ectopically silence *iab-6*. It is presumed that the same competition between positive and negative elements occurs in larger deletions like *Fab-7*^{1}; however, because the *iab-7* PRE is absent, the silenced state is unstable, leading to the activation of *iab-7*.

If boundaries ensure the functional autonomy of each BX-C *cis*-regulatory domain, one would expect to find elements separating each of them. To date only one other candidate boundary element, *Mcp*, has been identified. *Mcp* is located between *iab-4* and *iab-5* and is defined by three small deletions that span a prominent chromatin-specific nuclease hypersensitive region (Karch et al., 1994). Like *Fab-7*, the change in segmental identity induced by the *Mcp* mutations are easily recognized in adult males. Since the other abdominal segments have quite similar morphology, it is possible that mutations in other boundaries in the *Abd-B cis*-regulatory region would be too subtle to be recognized in genetic screens. In the studies reported here, we have a different strategy to identify and characterize the *Fab-8* boundary, which marks the distal end of the *iab-7* domain and is responsible for insulating *iab-7* from *iab-8*.

MATERIALS AND METHODS

P element transformation

Germline transformation was performed essentially as described in Mihaly et al. (1997). Plasmid DNA mixes were injected either in *ry*^{506} or *w*^{1118} host strains.

Generation of *Fab-8* mutations

In order to avoid gap repair by the homolog chromosome, the P element in *fs(3)5649* was mobilized over a chromosome carrying a deficiency for the distal part of BX-C (*Df(3)R59*; Gyurkovics et al., 1990) and the Δ2-3-producing transposase. Haplosterility of such *trans*-heterozygotes was covered by a duplication of BX-C on the X chromosome, *Dp(3:1)bxd*^{111}. Dysgenic males *fs(3)5649/Df(3R)R59, Δ2-3;Dp(3:1)bxd*^{111} were crossed to *TM2,ry/MKRS* females and putative deletion mutations were recognized on the basis of their *ry*$^{-}$ and/or dominant gain-of-function *Fab-8* phenotype. All putative mutations were analyzed by PCR with a set of oligonucleotide primers that hybridize on both sites of the P element. The endpoints of the deletions were sequenced.

Plasmid constructions

8XS is an 8 kb *Xho*I-*Sal*I fragment [coordinates 60,241-68,235 of the BX-C sequence from Martin et al. (1995)]. 8XSΔHSI-II is a derivative of 8XS in which the central *Hin*dIII-*Pst*I fragment (from 62,541 to 64,584) has been deleted. Both inserts were cloned upstream of the *Ubx-lacZ* reporter gene in vector 1204 (Simon et al., 1990) carrying the *rosy* gene selectable marker. All other 8XS constructs were inserted upstream of the *Ubx-lacZ* reporter gene in the CaSpeR*Ubx-lacZ* transposon vector (Qian et al., 1991). In 8XSλ, the *Hin*dIII-*Pst*I

fragment from coordinates 62,541 to 64,584 has been replaced by a 2 kb *Hin*dIII-*Pst*I fragment derived from bacteriophage λ. In 8XSΔHS1-2, the *Hin*dIII-*Pfl*M1 fragment from coordinates 63,384 to 64,584 has been deleted from the 8XS fragment. The 3.6XH fragment corresponds to the fragment *Xho*I-*Hin*dIII (64,584-68, 235) and the 2.1PP fragment corresponds to a 2.1 kb *Pst*I fragment from 60,451 to 62,380. In the enhancer-blocking assays, an *Afl*II fragment (62,380-65,210) was inserted between the *white* enhancer and the *mini-white* gene in the vector of Hagstrom et al. (1996). In subsequent constructs the *Eco*RI-*Afl*II fragment (62,380-63,788) covering the *iab-8 PRE* was inserted in the same *white* enhancer-*mini-white* vector, while the *Hin*dIII-*Eco*RI fragment spanning *Fab-8* (63,788-64,584) was inserted between the UPS-NE elements of the *ftz* enhancer and the *hsp-70-lacZ* reporter gene of Hagstrom et al. (1996). All cloning details are available upon request.

Antibody staining

Embryos were stained as described in Mihaly et al. (1997).

Preparation of larval and adult cuticles

Larval cuticles were prepared for microscopy following a procedure of Van der Meer (1977). In order to distinguish homozygous *Fab-8* mutant larvae, we used a TM3 balancer containing a duplication of the *yellow*$^{+}$ gene and constructed the following stocks: *y;Fab-8*^{64}*/TM3,y*$^{+}$ and *y;Fab-8*^{416}*/TM3,y*$^{+}$. Adult abdominal cuticles were mounted as described in Mihaly et al. (1997).

DNA techniques and chromatin digests

Whole genome Southern analysis were performed as described in Gyurkovics et al. (1990). Chromatin digests were isolated and analyzed by indirect end labeling as described in Galloni et al. (1993) and Karch et al. (1994). The DNA lesions of *Fab-8* mutations were recovered by PCR using Appligene Taq polymerase. PCR products were then cloned into pGEM-T vector system I (Promega) and sequenced using double-strand template with the USB Sequenase 2.0 system. PCR reactions were carried out on single flies according to Gloor et al. (1993).

RESULTS

Chromatin structure of the *iab-7*:*iab-8* junction

Previous studies have shown that the *Fab-7* boundary as well as the adjacent *iab-7* PRE are defined by prominent nuclease hypersensitive regions in chromatin digests (Galloni et al., 1993). We reasoned that if *iab-7* and *iab-8* are separated by a *Fab-8* boundary element, such an element should be marked by one or more nuclease hypersensitive regions. To investigate this possibility we examined the chromatin structure of the DNA segment on the distal side of the *iab-7 cis*-regulatory domain. Since the precise endpoints of the *iab-7 cis*-regulatory domain have not been previously defined, we focused our attention on the DNA segment near the most distal DNA lesion known to affect *iab-7* function, the R73 deletion (Gyurkovics et al., 1990). As shown in Fig. 1, the R73 deletion maps near the middle of an ~8 kb *Xho*I-*Sal*I fragment (8XS; coordinates 60,241-68,235 in BX-C in Martin et al., 1995). To analyze the chromatin structure of this DNA segment we used the indirect end labeling technique with probes abutting either the proximal XhoI site (see Fig. 2) or the distal *Sal*I site (not shown). The *Xho*I probe labels a ~20 kb fragment extending from within the *iab-7 cis*-regulatory domain distally towards *iab-8* and the 3′ end of the *Abd-B* transcription unit.

In DNaseI digests of KC cell nuclei (see Fig. 2), there are two major nuclease hypersensitive regions in the DNA segment just beyond the R73 deletion. The first of these, HS1, overlaps the distal edge of the R73 deletion and spans a DNA segment of ~400 bp. HS1 is flanked on both the proximal and distal sides by several weaker DNaseI cleavage sites. The second DNaseI hypersensitive region, HS2, is located ~1 kb distal and spans about 150 bp. The same pair of DNaseI hypersensitive regions is observed in digests of nuclei prepared from embryos. Additionally, these two DNA segments are hypersensitive to digestion by micrococcal nuclease. Equivalent results were obtained using a probe abutting the distal *Sal*I site (not shown).

Boundary and PRE activity

Although a variety of different regulatory elements are known to be marked by nuclease hypersensitive regions, we speculated that HS1 might correspond to the *Fab-8* boundary while the more distant hypersensitive region, HS2, might correspond to an *iab-8* PRE. Supporting the latter possibility is the finding that HS2 contains a ~12 bp sequence motif, which is present in several PREs in BX-C and elsewhere in the genome and is thought to be a binding site for the *Pc-G* protein *pleiohomeotic* (Brown et al., 1998; Mihaly et al., 1998). To test this idea, we inserted a ~2.8 kb *Afl*II restriction fragment from the middle of 8XS that encompasses both HS1 and HS2 (see Fig. 1) into a P-element transgene, w_e*-mini-white*, in between the *white* enhancer and the *mini-white* reporter (see Fig. 3). In previous studies, we used this same vector to analyze the *Fab-7* boundary and the adjacent *iab-7* PRE (Hagstrom et al., 1996, 1997). As was found for *Fab-7*-containing transgenes, nearly half of the w_e*-AflII-mini-white* lines showed evidence of enhancer blocking activity. In addition to the boundary activity, the *Afl*II fragment has a silencing activity and *mini-white* expression was silenced in about a quarter of the lines when the transgene insert was homozygous (Fig. 3C, see Hagstrom et al., 1997).

To further delimit the sequences conferring blocking and silencing activities, we subdivided the 2.8 kb *Afl*II into two smaller restriction fragments. The first is an ~800 bp *Hin*dIII-*Eco*RI fragment spanning HS1 and is expected to contain the *Fab-8* boundary (see Fig. 1). To test the HS1 fragment for boundary activity, we used a reporter construct in which the *fushi-tarazu* (*ftz)* UPS and NE enhancers drive β-galactosidase expression from an *hsp70 promoter-lacZ* fusion gene (Fig. 3). The UPS enhancer generates a pattern of seven stripes around blastoderm stage, while the NE enhancer activates expression in a subset of cells in the CNS during germ band extension. The *ftz* vector offers the advantage that it is less sensitive to chromosomal position effects than the w_e*-mini-white* assay system, and it is more readily possible to compare the blocking activity of different fragments. We examined the pattern of β-galactosidase expression in eight independent transgenic lines in which the putative *Fab-8* boundary element (the 800 bp *Hin*dIII-*Eco*RI fragment) is inserted between the *ftz* enhancers and the *hsp70* promoter. As illustrated for the *ftz* stripes in Fig. 3, we found that the blocking activity is equivalent to that of *Fab-7* boundary; stripe and CNS β-galactosidase expression was reduced to the same extent as that seen with *Fab-7*. We conclude from these results that the HS1 fragment has boundary activity.

The second fragment is a ~1.4 kb *Eco*RI-*Afl*II fragment, which spans HS2 and is expected to contain the *iab-8* PRE (see

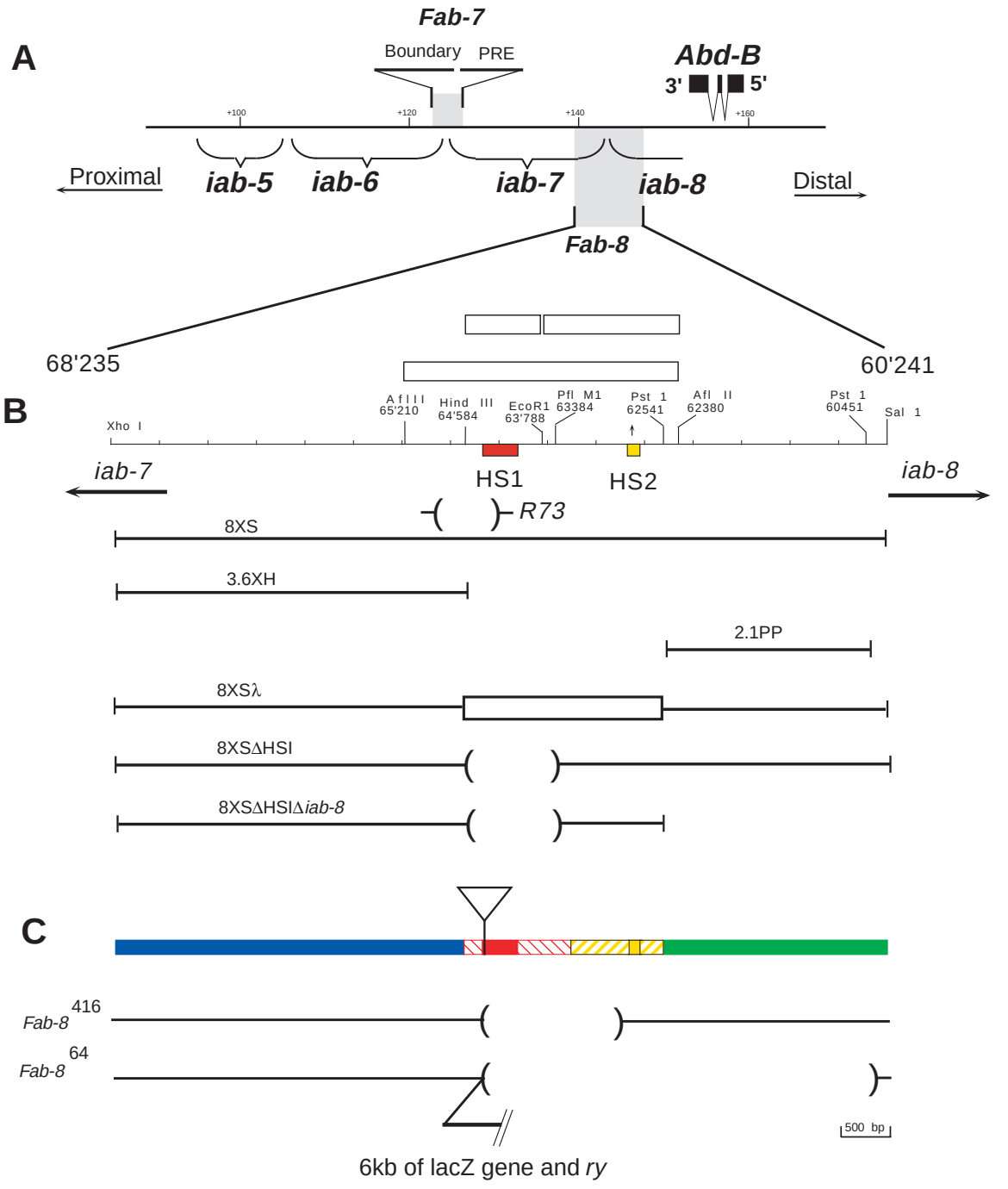

Fig. 1. (A) Distal part of the BX-C. The thin horizontal line represents the genomic DNA of the distal region of BX-C marked off in kilobases. The only class A *Abd-B* transcript that is required for morphogenesis in PS10 to 13 is shown below the DNA line (Zavortink and Sakonju 1989; Celniker et al., 1990). The horizontal brackets below the DNA indicate the extents of *iab-5*, *iab-6*, *iab-7* and *iab-8* (the beginning of the *iab-8* domain is placed according to the data presented in this paper). The *Fab-7* boundary is indicated above the DNA line. The 8 kb *Xho*I-*Sal*I fragment (8XS) used in this study is drawn below the DNA line. Proximal points towards the centromere, while distal indicates the direction of the telomere. (B) The 8XS fragment and its derivatives. The 8XS fragment is marked every 500 bp. Restriction sites used to generate the 8XS derivatives are indicated with their coordinate in the BX-C sequence of Martin et al. (1995; see Materials and Methods). The two nuclease hypersensitive regions, HS1 and HS2, are shown by the red and yellow boxes, respectively. While the fragments used for the enhancer blocking and PRE assays are indicated by the boxes above the 8XS restriction map, the 8XS derivatives used with the *Ubx-lacZ* reporters are drawn below. At the bottom is a colored version of 8XS that indicates the different DNA segments in this fragment; this colored version is used for reference in several of the subsequent figures. The insertion site for the P[*ry lacZ*] transposon in *fs(3)5649* is indicated (the insertion point was sequenced by Sue Celniker and Ed Lewis, personal communication). (C) *Fab-8* boundary deletions in the context of the BX-C. The extent of the *Fab-8* deletions recovered after mobilization of the *fs(3)5649* transposon are indicated at the same scale as in Fig. 1B. In *Fab-8*^{64}, a 6 kb DNA fragment from the transposon remains; it contains the *lacZ* reporter gene and part of *ry*$^{+}$.

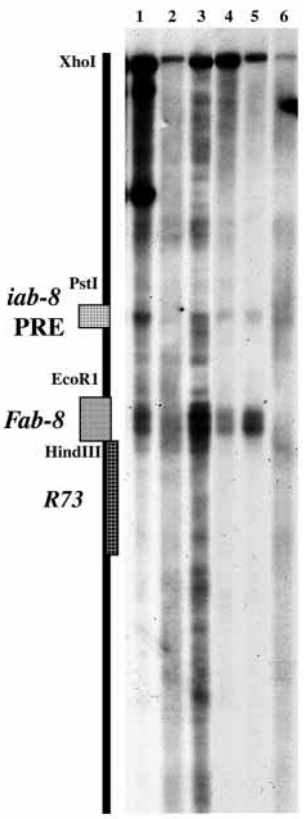

Fig. 2. Chromatin structure distal to the R73 deletion. Autoradiograph is an indirect end-labeling analysis of the chromatin structure of junction between *iab-7* and *iab-8*. DNA prepared from DNaseI and micrococcal nuclease digests of chromatin or naked DNA was restricted with *Xho*I. After electrophoresis and blotting, the nitrocellulose filter was probed with a ~1 kb *Eco*RI-*Xho*I fragment abutting the *Xho*I site on the proximal side of the 8XS restriction fragment (see Fig. 1). This displays the nuclease cleavage sites reading from within *iab-7* through the region deleted in R73 (see Fig. 1) distally into *iab-8* and and the 3′ end of the *Abd-B* transcription unit. The location of HS1, and HS2 are indicated. Lanes from right to left are: (1) DNaseI digest of 12-24 hours embryonic nuclei. The dark band above HS2 is from a restriction site polymorphism in the embryonic genomic DNA. (2) Micrococcal nuclease digest of naked KC cell DNA. (3) Micrococcal nuclease digest of nuclei from KC cells. (4) DNaseI digest of nuclei from KC cells. (5) DNaseI digest of nuclei from KC cells. (6) DNaseI digest of naked DNA from KC cells.

Fig. 1). We used the w_e-*mini-white* vector to test whether it has PRE activity. As indicated in Fig. 3, we found that the HS2 fragment functions as a PRE, and 5 out 14 transgenic lines showed pairing-sensitive silencing.

The *Fab-8* boundary separates *iab-7* and *iab-8* initiation elements

The results described in the previous section are consistent with the hypothesis that the HS1 fragment corresponds to the *Fab-8* boundary, while the HS2 fragment corresponds to an *iab-8* PRE. If this model is correct, then sequences in 8XS located proximal to the *Fab-8* boundary (see Fig. 1) should be derived from *iab-7*, and hence might contain regulatory elements that are responsible, at least in part, for specifying the PS12 expression pattern of *Abd-B*. Similarly, sequences in 8XS distal to the putative boundary should be derived from *iab-8* and might contain, in addition to the *iab-8* PRE, elements that specify the PS13 expression pattern of *Abd-B*. To test this prediction, we asked whether sequences on each side of the boundary will drive expression of a *Ubx* promoter-*lacZ* reporter construct in the expected parasegmental pattern. On the proximal side we used a 3.6 kb *Xho*I-*Hin*dIII fragment (3.6XH), while on the the distal side, we used a 2.1 kb *Pst*I fragment (2.1PP) which is located just beyond HS2. The β-galactosidase expression pattern observed for each transgene indicates that the *Fab-8* boundary is flanked on the proximal side by elements which can function as *iab-7* initiators and on the distal side by elements that can function as *iab-8* initiators.

During the initiation phase the 3.6XH *Ubx-lacZ* transgenic lines typically express low levels of β-galactosidase in PS12 and in PS 14. As can be seen in the germband extended embryo

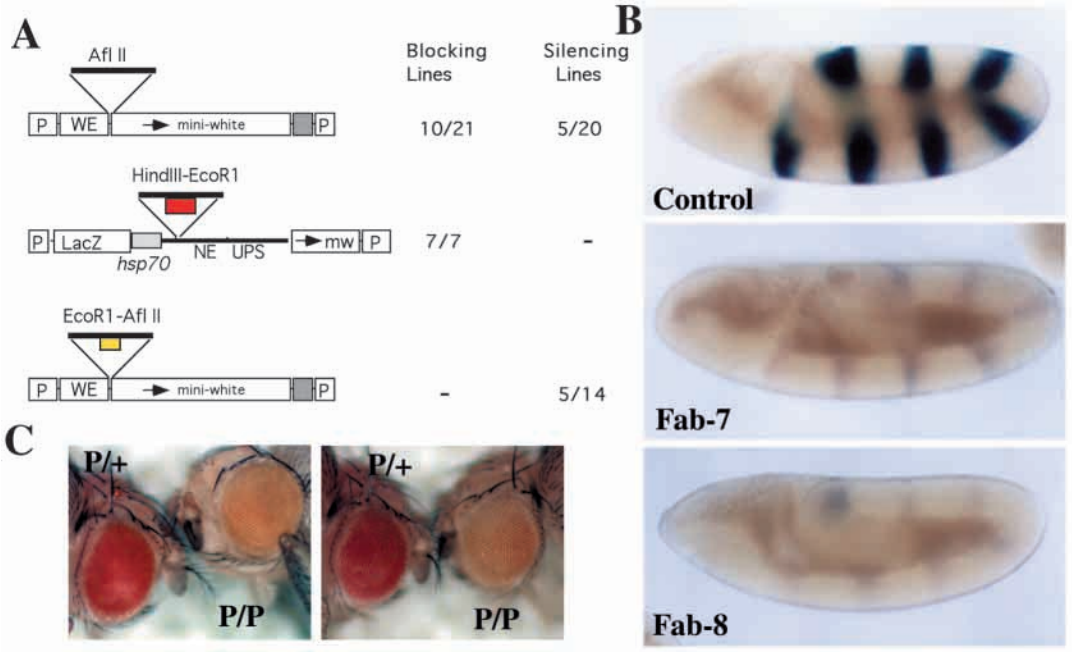

Fig. 3. Enhancer blocking and silencing activities associated with HS1 and HS2. (A) The structure of the transgenes, w_e-*mini-white* and *ftz-hsp70:lacZ*, used to assay enhancer blocking and silencing activities of restriction fragments containing HS1 and/or HS2. The number of lines showing enhancer blocking and pairing-dependent silencing activity is indicated on the right of the first *Afl*II construct. In the second construct, the *Hin*dIII-*Eco*RI fragment containing only HS1 blocks interactions between the *ftz* enhancers (NE and UPS) and the *hsp70* promoter in all 7 transformant lines tested. In the third construct, an *Eco*RI-*Afl*II fragment containing HS2 was inserted into the w_e-*mini-white* vector as indicated. The number of lines showing pairing-sensitive silencing is indicated. (B) Control. The *ftz* UPS enhancer (see A) drives β-galactosidase expression in a stripe pattern in early embryos. When *Fab-7* or *Fab-8* are placed between the *ftz* enhancers and the *hsp70:lacZ* fusion gene, they block to a similar level the stripe (and CNS: not shown) expression. (C) Pairing-sensitive silencing. The two photographs in C show the eye color of two independent transgenic lines heterozygous and homozygous for the w_e-*Eco*RI-*Afl*II-*mini-white* construct.

in Fig. 4A, this *iab-7*-like pattern is superimposed upon the basal activity of the *Ubx* promoter, which gives β-galactosidase expression in the head and in stripes in the lateral side of the epidermis (Simon et al., 1990). PS12 expression in the epidermis is not maintained at later stages of embryogenesis and disappears by the completion of germband retraction. At the same time, relatively high levels of β-galactosidase appear in a group of cells in the CNS, in cells along the line of the dorsal closure and in group of cells that form the tracheal placode (Fig. 4A). These results argue that the 3.6XH fragment contains *iab-7* initiators and cell/tissue-specific enhancers, but no functional PRE.

The initial pattern of β-galactosidase expression for the 2.1PP *Ubx-lacZ* transgenic lines differs in two respects from that of the 3.6XH *Ubx-lacZ* lines. First, the 2.1PP drives much higher levels of β-galactosidase expression. Second, and more importantly, the anterior limit is PS13 not PS12. At the early stage shown in Fig. 4A, the β-galactosidase expression is observed in the ectoderm and mesoderm of PS13 and in more posterior parasegments. Like the 3.6XH transgene, the parasegment-specific β-galactosidase expression pattern is not properly maintained, and either spreads anteriorly or fades away altogether during the maintenance phase. Thus, the 2.1PP fragment contains *iab-8* initiators, but no PRE.

The regulatory activities of the 8XS fragment depend upon its orientation relative to the *Ubx-lacZ* reporter

Since the *iab-7* and *iab-8* initiators in the 8XS fragment are separated by the *Fab-8* boundary (and the *iab-8* PRE), we reasoned that the 8XS fragment might generate different parasegmental expression patterns depending upon its orientation relative to the *Ubx-lacZ* reporter gene. To test this possibility, we inserted 8XS into the *Ubx-lacZ* reporter so that either the proximal *iab-7* (the 8XS:*iab-7* transgene in Fig. 4B) or the distal *iab-8* (the 8XS:*iab-8* transgene in Fig. 4B) sequences are located close to the promoter. As anticipated, the pattern of β-galactosidase expression in transgenic embryos depends upon which initiator elements are next to the promoter.

When the *iab-7* sequences are adjacent to the *Ubx* promoter (8XS:*iab-7*), the expression pattern is indistinguishable from that observed for the 3.6XH transgene (compare Fig. 4A and 4B). During the initiation phase, the 8XS:*iab-7* transgene gives β-galactosidase expression in PS12 (and PS14); however, in spite of the fact that the 8XS fragment contains *iab-8* initiators, these regulatory elements do not seem to activate the *Ubx* reporter and no expression is observed in PS13. As was found for the 3.6XH transgene, the *iab-7*-like pattern fades during the maintenance phase, and is replaced by β-galactosidase expression in the CNS and trachea. This result implies that the *iab-8* PRE (present in this 8XS fragment) is unable to sustain the β-galactosidase expression pattern initiated by the *iab-7* regulatory elements in PS12.

When the *iab-8* sequences from 8XS are adjacent to the *Ubx* promoter (8XS:*iab-8*), the expression pattern during the initiation phase is the same as that observed for the 2.1PP transgene; β-galactosidase is expressed at high levels in PS13, while there is no expression in PS12. However, the 8XS:*iab-8* transgene differs from the 2.1PP transgene in expression as it is maintained in PS13 and more posterior parasegments at later stages of development (compare Fig. 4A and B). This difference presumably reflects the activity of the *iab-8* PRE, which is missing from the 2.1PP fragment. To confirm that the maintenance activity of the 8XS:*iab-8* transgene is due to the presence of a PRE, we examined the effects of a *Polycomb* mutation on β-galactosidase expression. We found that the PS13-limited expression pattern is not maintained in the absence of *Pc* function, and β-galactosidase expression spreads into the anterior of the embryo (data not shown).

The *Fab-8* boundary confers the orientation dependence of the 8XS fragment

A plausible explanation for the different parasegmental expression patterns of the 8XS:*iab-7* and 8XS:*iab-8* transgenes is that only regulatory elements proximal to the *Fab-8* boundary in each transgene are allowed to interact with the *Ubx-lacZ* reporter, while interactions with regulatory elements distal to the boundary are blocked. If this explanation is correct, then this orientation dependence should disappear when the *Fab-8* boundary is removed. Alternatively, the distal regulatory elements in each orientation may simply be too far from the *Ubx* promoter to control its activity. To distinguish between these possibilities, we generated two different types of 8XS transgenes. In the first, 8XSΔHS1-2, we deleted a 2 kb fragment spanning HS1 and HS2; this deletion, 8XSΔHS1-2, is expected to remove both the *Fab-8* boundary and the *iab-8* PRE (see Fig. 1). The 8XSΔHS1-2 deletion fragment was then inserted in either orientation upstream of the *Ubx-lacZ* reporter to give 8XSΔHS1-2:*iab-7* or 8XSΔHS1-2:*iab-8*. In the second type of transgene, 8XSλ, we replaced the 2 kb HS1-2 fragment with a 2 kb fragment from bacteriophage λ. The 8XSλ fragment was also inserted in either orientation upstream of the *Ubx-lacZ* reporter to give 8XSλ:*iab-7* and 8XSλ:*iab-8*.

If the *Fab-8* boundary, and not the distance, is responsible for the orientation dependence, then the expression pattern of all four of these transgenes should be identical. This is the case. As shown in Fig. 5A for the 8XSλ pair, the initial expression pattern is the same as that observed for 8XS:*iab-8* (see Fig. 4B). There is no expression in PS12, instead, high levels of β-galactosidase are found in the epidermis and mesoderm of PS13 and PS14 (compare 8XSλ:*iab-7* and 8XSλ:*iab-8*). This result indicates that the initial activation of the *Ubx-lacZ* reporter is under the control of the *iab-8* and not the *iab-7* initiators. During the maintenance phase, all four transgenes also give the same expression patterns; however, in contrast to the early pattern, the late pattern is reminiscent of that seen for the 8XS:*iab-7* transgene (or for 3.6XH), and not the 8XS:*iab-8* transgene. First, the PS13-specific anterior border of expression is lost, indicating that these four transgenes do not have functional PRE. This was expected since the fragment containing HS2, which had PRE activity, is deleted from both 8XSΔHS1-2 and 8XSλ. Second, β-galactosidase is expressed in the tracheal placode, along the dorsal closure and in cells in the CNS, suggesting that, in the absence of the boundary and the PRE, the regulation of the *Ubx:lacZ* reporter switches from the early initiators in the *iab-8* DNA segment to the late cell/tissue-specific enhancers in the *iab-7*DNA segment.

Although these results are consistent with the model in which the *Fab-8* boundary confers orientation dependence on 8XS fragment by blocking the action of distal regulatory elements, there is one potential caveat. The deletion in both 8XSΔHS1-2 and 8Xλ removes not only the boundary but also

the *iab-8* PRE. Hence, it was important to examine the orientation dependence of a deletion, 8XSΔHS1, that removes only HS1 and should eliminate just *Fab-8* boundary function. Fig. 5B shows the β-galactosidase expression pattern of the 8XSΔHS1:*iab-7* and 8XSΔHS1:*iab-8* transgene pair. Like the 8XSΔHS1-2 and the 8XSλ transgene pairs, the 8XSΔHS1 fragment drives β-galactosidase expression with an anterior limit of PS13 irrespective of its orientation relative to the *Ubx-lacZ* reporter. Thus when just the boundary is removed, the *iab-8* initiators in 8XS control the initial activation of the *Ubx* promoter even when they are farther from the promoter than the *iab-7* initiators. The two 8XSΔHS1 transgenes differ from the transgenes carrying the larger deletions 8XSΔHS1-2 and 8XSλ in that they retain maintenance activity (compare Fig. 5A and B). For both 8XSΔHS1 transgenes, the anterior limit of PS13 set during the initiation phase is maintained later in development. This result confirms our mapping of the *iab-8* PRE to the fragment containing HS2 and demonstrates that this PRE is not responsible for the orientation dependence of the 8XS fragment. In addition, the late cell type-specific expression of the *Ubx-lacZ* reporter in the trachea and CNS observed in the two larger deletions 8XSΔHS1-2 and 8Xsλ is suppressed in 8XSΔHS1 (compare Fig. 5A and 5B). This result indicates that these late *iab-7* cell/tissue enhancers are inactivated by the *iab-8*PRE when the boundary is deleted.

The *Fab-8* boundary restricts the realm of action of the *iab-8* PRE

Besides demonstrating that *Fab-8* boundary blocks distal initiators, the results described in the previous sections suggest that the boundary may also restrict the action of the *iab-8* PRE. First, when the *Fab-8* boundary is present, the PRE is unable to maintain the PS12 expression pattern initiated by the 8XS:*iab-7* transgene. Second, the boundary prevents the PRE from inactivating the cell/tissue-specific enhancers in the *iab-7* 3.6XH DNA segment. To test this suggestion further, we inverted the restriction fragment in 8XS, which contains the *Fab-8* boundary and the *iab-8* PRE (8XS-IN in Fig. 5C). We reasoned that this inversion should alter the realm of action of the *iab-8*PRE so that it now functions to maintain the *Ubx-lacZ* expression pattern activated by the *iab-7* instead of the *iab-8* initiators. Effectively, at early stages, the pattern of expression of the 8XS-IN:*iab-7* and 8XS-IN: *iab-8* transgenes is the same as their parental counterparts 8XS:*iab-7* and 8XS:*iab-8* (compare Fig. 4B with 5C). However, the PS12 expression pattern initiated by *iab-7* elements in the 8XS-IN:*iab-7* transgene is maintained, while the PS13 pattern initiated by the *iab-8* elements in 8XS-IN:*iab-8* is not maintained (see Fig. 5C). Additionally, as was the case for the boundary deletion, the late cell/tissue-specific expression in the trachea and CNS is repressed in the 8XS-IN:*iab-7* transgene.

The *Fab-8* boundary blocks PS12 repressors in the *iab-8* initiator

One unexpected finding was that the *iab-7* initiators in the 8XS fragment appear to be inactivated when the boundary (or the boundary plus the PRE) is deleted (see Fig. 5A and B). In fact, even when the *iab-7* initiators adjoin the *Ubx-lacZ* reporter, all of the 8XS boundary deletion constructs drive expression in PS13 but not in PS12. This suggests that negative regulatory elements or repressors in the *iab-8* initiator can inactivate the *iab-7* initiator at a distance when the *Fab-8* boundary is deleted. This model predicts that PS12 expression should be restored in the boundary deletion, 8XSΔHS1, by removing the distal DNA segment containing the *iab-8* initiator. This prediction is correct. As can be seen in Fig. 5D, the double deletion, 8XSΔHS1Δ*iab-8* drives β-galactosidase expression in PS12 (and PS14) early in development. Since the double deletion retains the DNA segment containing the HS2- *iab-8* PRE, β-galactosidase expression should be maintained with an anterior limit of PS12 later in development. This is also the case (see Fig. 5D).

Isolation of *Fab-8* mutations in the context of BX-C

The transgene assays described above provide strong evidence that the 8XS fragment spans the junction of the *iab-7* and *iab-8 cis*-regulatory domains and contains not only parasegment-specific initiators but also the *Fab-8* boundary and an *iab-8*PRE. However, it was important to confirm the conclusions drawn from these transgene experiments by examining the functions of this DNA segment in the context of BX-C itself. For this purpose we took advantage of an enhancer trap, *fs(3)5649* isolated by L.Cooley which is inserted into the BX-C near the proximal edge of HS1, and hence should be located just within the *iab-7 cis*-regulatory domain (see Fig. 6). According to our model, the *fs(3)5649* enhancer trap should behave like the previously characterized *Bluetail* transposon, which is inserted on the opposite (proximal) side of the *iab-7 cis*-regulatory domain (Galloni et al., 1993); it should be subject to regulatory elements located within *iab-7*, but not to regulatory elements in the adjacent *cis*-regulatory domains. Like *Bluetail*, the *fs(3)5649* transgene should be insulated from the *iab-6* regulatory elements by the *Fab-7* boundary. Similarly, on the distal side, it should be protected from regulatory elements in *iab-8* by the *Fab-8* boundary. Fig. 6 shows the expression pattern of the *fs(3)5649* enhancer trap line. During the initiation phase, high β-galactosidase levels are observed in PS12 and in the posterior part of PS14. There is also expression in a row of cells localized laterally in PS13. At later stages of development the PS12 pattern is maintained while expression in more posterior parasegments is lost.

We next mobilized the *fs(3)5649* transposon to generate imprecise excisions that remove the *Fab-8* boundary and/or other flanking sequences. Two imprecise excisions extending distally from the transposon insertion site were characterized. The first, *Fab-8*^{416}, removes the *Fab-8* boundary but not the *iab-8* PRE. As was observed for deletions in the *Fab-7* region, which remove the *Fab-7* boundary, but not the *iab-7* PRE, the *Fab-8*^{416} deletion exhibits a mixture of gain-of-function and loss-of-function phenotypes. In adult mutant females, the gain-of-function transformation of A7 to A8 can be seen on the dorsal side by the partial absence of tergite in A7 (see Fig. 7A). This segmental transformation is that expected for the ectopic activation of *iab-8* in PS12/A7, where it would direct *Abd-B* expression in a pattern appropriate for PS13. The loss-of-function transformation of A7 into A6 can be seen on the ventral side by the shape of the hairs of the sternite. This mixture of gain- and loss-of-function phenotypes can be explained by a fusion of the *iab-7* and *iab-8 cis*-regulatory domains. In PS12/A7 there is a competition between ectopic activation of the fused domain by positive regulatory elements in *iab-7* and silencing of the fused domain by negative

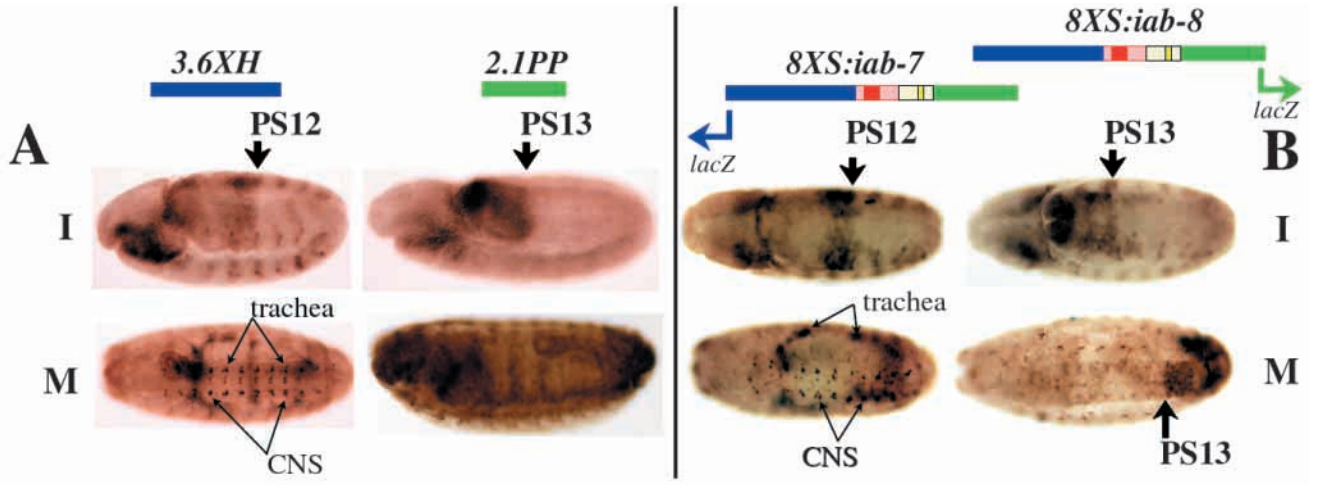

Fig. 4. The 8XS fragment drives a *lacZ* expression pattern which is orientation dependent. Above each panel the different constructs are indicated in colors similar to the 8XS fragment shown in Fig. 1. All embryos are shown with the anterior pole on the left and the dorsal side on top. The top row of each panel contains early embryos at the stage of extended germ band during the inititiation phase of BX-C regulation (I). The bottom row shows late embryos during the maintenance phase of BX-C regulation (M). (A) β-galactosidase expression pattern driven by the 3.6XH (four out of five transformant lines) and 2.1PP fragments (five out of six transformant lines). The parasegmental anterior borders of β-galactosidase expression are shown by vertical thick arrows. The late expression patterns in the CNS and tracheal placodes are labelled (see text). (B) The 8 kb *Xho*I-*Sal*I fragments (8XS) are represented at the top. The embryos on the left show the *lacZ* expression pattern driven by 8XS:*iab-7*, where the *lacZ* gene is next to the *iab-7* side (four out of six transformant lines show this pattern). The embryos on the right show the *lacZ* expression pattern driven by 8XS:*iab-8* where the *lacZ* gene is adjacent to the *iab-8* side. The early PS13/PS14 expression pattern as well as the maintenance was observed in all five transformant lines obtained with this construct. However, only one line gave very strong maintenance in the CNS as shown in this panel.

regulatory elements in *iab-8*. If the fused domain is activated, then *Abd-B* expression in PS12/A7 is driven by *iab-8*, specifying PS-13/A8 segmental identity. If the fused domain is silenced, turning off both *iab-7* and *iab-8*, then *Abd-B* expression in PS12/A7 is driven by *iab-6*, specifying a PS11/A6 segmental identity.

The larger deletion, *Fab-8*^{64}, extends from a site within the *fs(3)5649* transposon to 250 bp near the distal edge of the 8XS restriction fragment (see Fig. 1), removing the *Fab-8* boundary (HS1) *iab-8* PRE (HS2) and much of the *iab-8* initiator in 8XS (though there must be other *iab-8* initiators distal to the breakpoint that remain intact: see in Gyurkovics et al., 1990). Like deletions in the *Fab-7* region that remove both the *Fab-7* boundary and the *iab-7* PRE, *Fab-8*^{64} exhibits only a gain-of-function phenotype. The transformation of PS12 into PS13 can be seen on both the ventral and dorsal sides of the first instar (Fig. 7B) and third instar larval ectoderm (Fig. 7C) and in the cuticle of adult females (see Fig. 7A). Though a competition between ectopic activation and silencing in the fused *iab-7*-*iab-8* regulatory domain probably still occurs in this deletion, the balance is apparently shifted towards activation. This could be due, at least in part, to the removal of the repressors that seem to be associated with the *iab-8* initiators in the 8XS fragment (see above). In addition, it is also likely that the silenced state cannot be properly maintained in the absence of the *iab-8* PRE.

Further evidence that the insulating activity of the *Fab-8* boundary is responsible for ensuring the functional autonomy of the *iab-7* and *iab-8 cis*-regulatory domains comes from an analysis of the β-galactosidase expression pattern of the *Fab-8*^{64} deletion. While the *ry* marker is lost in the *Fab-8*^{64} deletion, it retains a functional *lacZ* gene. As shown in Fig. 6, the deletion alters the pattern of β-galactosidase expression pattern. Unlike the parental transposon, the *Fab-8*^{64} deletion variant expresses high levels of β-galactosidase not only in PS12 and PS14, but also in PS13. Moreover, expression in PS12 and PS13 is maintained at a high level at late stages of development. This is the result expected if the *lacZ* reporter is subject to the regulatory influences of the *iab-8 cis*-regulatory domain in the *Fab-8*^{64} deletion mutant.

DISCUSSION

In the studies reported here, we have investigated the mechanisms that ensure the functional autonomy of two BX-C *cis*-regulatory domains, *iab-7* and *iab-8*. These two domains regulate the *Abd-B* gene and are responsible for specifying segmental identity in PS12 and PS13, respectively. We show that *iab-7* and *iab-8* are separated by a chromatin domain boundary element, *Fab-8*. In transgene assays, the *Fab-8* boundary can block enhancer:promoter interactions and restrict the realm of action of the *iab-8*PRE. We demonstrate that *Fab-8* is essential in BX-C for the proper specification of segmental identity in PS12. When the boundary is deleted, the *iab-7* and *iab-8 cis*-regulatory domains fuse into a single domain resulting in the misspecification of cell identity in PS12 as either PS13 or PS11. Our conclusions are supported by a recent independent study of Zhou et al. (1999) who have used completely different transgene assays to identify *iab-7* and *iab-8* regulatory elements and the *Fab-8* boundary.

While *Fab-8* marks the distal end of the *iab-7* domain, the proximal end is defined by a previously identified boundary element *Fab-7* (Hagstrom et al., 1996; Zhou et al., 1996; Mihaly et al., 1997). Like *Fab-8*, *Fab-7* has an essential insulator function in vivo and is required to protect *iab-7* from

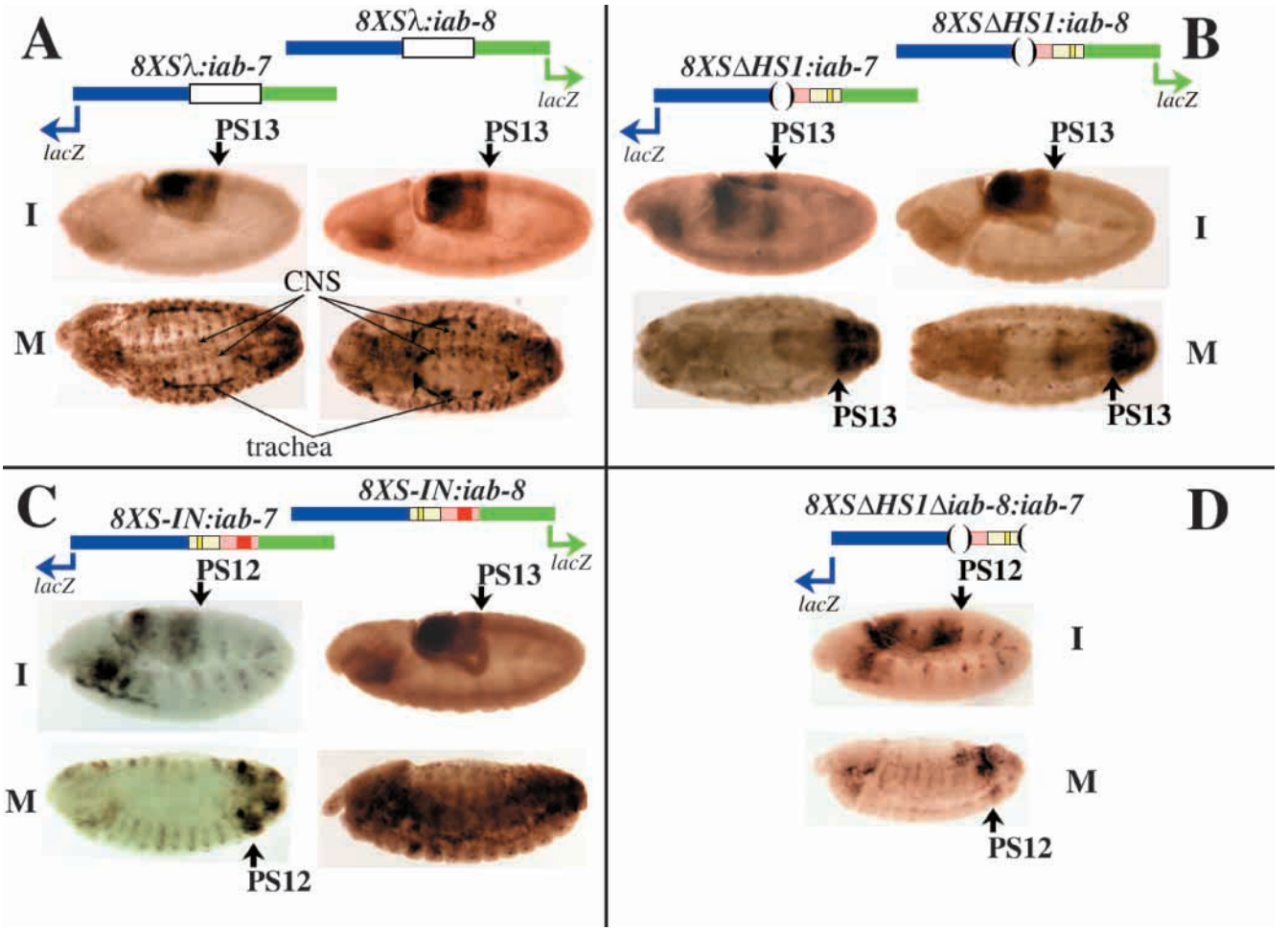

Fig. 5. *Fab-8* boundary deletions lead to the loss of orientation dependence of *lacZ* expression of 8XS. (A) The structure of the 8XS fragment in which the central *Hin*dIII-*Pst*I fragment is replaced by a fragment of similar size from bacteriophage λ is shown on top of the figure (see text and Fig. 4 legend). Similar patterns are observed in three out of three transformant lines obtained with 8XSλ:*iab-7* and all four lines obtained with 8XSλ:*iab-8*. (B) Fragment 8XSΔHS1 in which the *Fab-8* boundary is deleted is shown on top. All three transformant lines obtained with 8XSΔHS1:*iab-7* show the same expression pattern. With 8XSΔHS1:*iab-8*, one line out of three shows the strong maintenance in the CNS. (C) The structure of 8XS-IN in which the central *Hin*dIII-*Pst*I fragment containing the *Fab-8* and *iab-8*PRE has been inverted is drawn on top. These patterns are observed in all four transformant lines recovered with 8XS-IN:*iab*-7 and all eight transformant lines recovered with 8XS-IN:*iab-8*. (D) The structure of the fragment 8XSΔHS1Δ*iab-8* carrying the deletion of the region containing the PS13 initiator is shown on top. The same expression pattern is observed in all four transformant lines recovered with this construct.

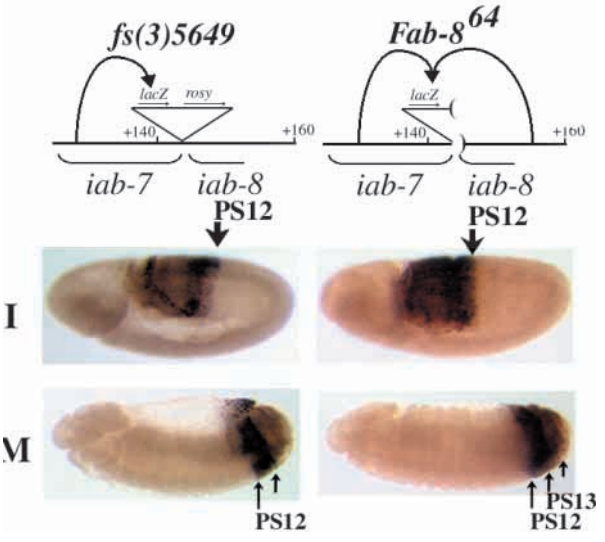

the adjacent proximal domain, *iab-6*. Together, the *Fab-7* and the *Fab-8* boundaries delimit the *iab-7* domain, ensuring its functional autonomy by shielding the domain from the regulatory influences of the neighboring *iab-6* and *iab-8* domains. Thus, *iab-7* represents the first example of a genetically defined higher order chromatin domain in a multicellular eukaryote.

Recent studies in yeast have shown that the transcriptionally repressed HMR locus is flanked by elements that function to delineate a silenced chromatin domain (Donze et al., 1999). These elements block the spread of silenced chromatin, protecting neighboring genes from repression by the SIR silencing complex assembled at HMR. The *Fab-7* and *Fab-8*

Fig. 6. β-glactosidase expression in *fs(3)5649* and *Fab-8*^{64}. The β-galactosidase expression patterns driven by the P[*ry*$^{+}$ *lacZ*] transposon in *fs(3)5649* and *Fab-8*^{64}are shown in early and late embryos (I and M).

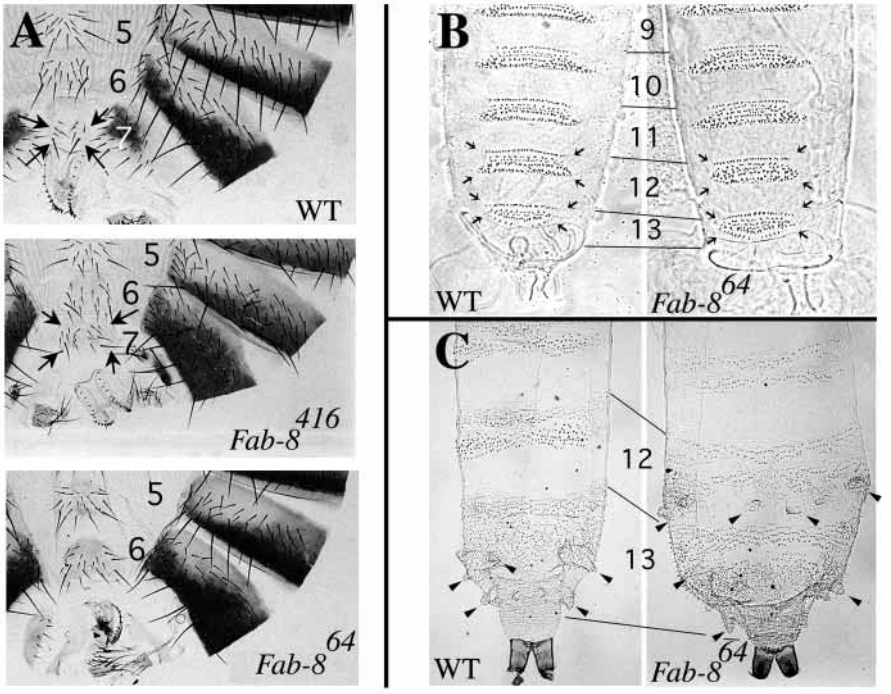

Fig. 7. Larval and adult phenotypes of *Fab-8* mutations. (A) Since A7 and A8 do not contribute to any visible cuticle after metamorphosis in males, there is no visible phenotype in adult males homozygous for the *Fab-8* deletion. The A7-to-A8 transformation is, however, clearly visible in females where A7 develops. Female abdomens were cut along the dorsal midline and flattened on a slide. The dorsal surface of each abdominal segment has a rectangular plate of hard cuticle called the tergite. Only half of the tergites of the 5th, 6th and 7th abdominal segments (numbered) are visible on the right of each panel, as well as the genitalia at the bottom (A8 is represented by a rudimentary unpigmented tergite). The ventral surface of abdominal segments is composed of soft cuticle called the pleura. On the ventral midline of the pleura, there are small plates of harder cuticle called sternites. In wild type, the 7th sternite can be easily distinguished from the more anterior sternites by its different shape and by the few bristles that are pointed towards the midline (arrows). While there is no sign of an 8th sternite, it is believed that the vaginal plate cells have A8 origin. *Fab-8*^{64} homozygous females clearly show segmental transformations. The 7th tergite is nearly absent and resembles the 8th tergite both in size and in the fact that it is unpigmented. The 7th sternite seen in wild-type females with its characteristic bristles is absent. Instead, we occasionally observe the appearance of thorn bristles, normally found on the vaginal plate, in place of the 7th sternite bristles (data not shown). In homozygous *Fab-8*^{416} females, cells in A7 show a mixture of two identities. On the dorsal surface, they have A8 identity as revealed by the absence of the 8th tergite. On the ventral side is a sternite. The organization and orientation of the bristles in this sternite resemble that normally found in more anterior sternites. (B) Ventral surface of the posterior parts of a WT and *Fab-8*^{64} first instar larva. Each abdominal parasegment (numbered) is covered by rows of seta belts of trapezoidal shape. The number of rows as well as their length increases in more posterior parasegments to reach the largest trapeze in PS12 (the PS12 and PS13 seta belts are indicated by arrows). PS13 can be distinguished from more anterior parasegments, because of the rectangular shape of the setal belt. In *Fab-8*^{64} homozygous larvae, the transformation of PS12 into PS13 is visible by the appearance of a setal belt of rectangular shape in PS12. (C) Dorsal sides of a WT and *Fab-8*^{64} homozygous 3rd instar larvae. In the posterior part of PS13 of WT larvae, a number of sensory organs specific to this parasegment are present (arrowheads). The transformation of PS12 into PS13 in *Fab-8*^{64} is revealed by the presence of these sensory organs in the posterior part of PS12.

boundaries perform an analogous function, restricting the action of *Pc-G* silencing complexes; however, they not only prevent silencing complexes assembled in the *iab-7* domain from 'spreading' to adjacent domains, they also protect the *iab-7* domain from the effects of silencing complexes in adjacent domains.

Boundary functions of *Fab-8* in transgene assays

In the context of BX-C, the primary role of the *Fab-8* boundary is to prevent adventitious interactions between regulatory elements (parasegment initiators/repressors, cell/tissue-specific enhancers and PREs) in adjacent *cis*-regulatory domains. Except for enhancer trap insertions like *fs(3)5649*, the boundary does not normally function to block interactions between these regulatory elements and promoters. However, our transgene assays, as well as those of Zhou et al. (1999) reveal that the boundary activities of *Fab-8* closely resemble those described for other insulators (Gerasimova and Corces 1996; Geyer 1997). When interposed between an enhancer and a promoter, the *Fab-8* boundary blocks enhancer:promoter interactions. This insulating activity is not specific to regulatory elements derived from BX-C; the *Fab-8* boundary can block interactions between enhancer:promoter combinations that are derived from other completely unrelated loci. The insulating activity also appears to be 'constitutive'; it can be detected both in early blastoderm embryos and in adult flies and exhibits no apparent stage or tissue specificity. In addition to blocking the action of positive regulatory elements, the *Fab-8* boundary can restrict the activity of elements that function as repressors or silencers. These negative elements include a silencer associated with the *iab-8* initiator that inactivates the *iab-7* initiator, and a *Polycomb* Response Element, the *iab-8*PRE. Finally, like other insulators, the *Fab-8* boundary is associated with a nuclease hypersensitive region.

Boundary functions of *Fab-8* during the BX-C initiation phase

During the initiation phase, the products of the gap and pair-rule genes select parasegmental identity by setting the activity state of the individual BX-C *cis*-regulatory domains. For example, the combination of gap and pair-rule gene products present in cells that give rise to PS12 set the *iab-7* domain in the active state, while they set the *iab-8* domain in the inactive state. To properly specify parasegmental identity, the *cis*-regulatory domains must function autonomously during this phase and there must be no cross-talk between initiator elements in adjacent domains. Our results indicate that the *Fab-8* boundary plays a critical role in establishing the functional

independence of the *iab-7* and *iab-8 cis*-regulatory domains, blocking adventitious interactions between the initiators in these two domains. This conclusion is supported by several lines of evidence.

The first comes from studies on the regulatory activities of the *iab-7* and *iab-8* initiators in the 8XS restriction fragment. When the *Fab-8* boundary is present, the regulatory activities of the 8XS fragment are determined by its orientation relative to the *Ubx-lacZ* reporter; only the initiator proximal to the boundary is able to activate the reporter, while the initiator distal to the boundary can not. When the boundary is removed from the 8XS fragment, orientation dependence is lost. The *iab-8* initiator drives *Ubx-lacZ* expression in PS13 and represses the *iab-7* initiator in PS12. Second, deletion of the *Fab-8* boundary in BX-C changes the pattern of β-galactosidase expression of the *fs(3)5649* enhancer trap. When the boundary is present, the enhancer trap is under the control of the *iab-7 cis*-regulatory domain and is expressed at high levels in PS12 during the initiation phase. When the boundary is deleted, high levels of β-galactosidase expression are observed not only in PS12 but also throughout PS13. Finally, the proper specification of PS12 identity depends upon the *Fab-8* boundary. When the boundary is deleted positive elements in *iab-7* can ectopically activate *iab-8* in PS12, transforming identity from PS12 to PS13. Conversely, negative elements in *iab-8* can ectopically repress *iab-7* in PS12. In this case, PS12 identity is transformed to PS11 because only *iab-6* remains active in the presumptive PS12 cells.

Boundary functions of *Fab-8* during the BX-C maintenance phase

In addition to preventing cross talk between regulatory elements in *iab-7* and *iab-8* during the initiation phase, our results indicate that the *Fab-8* boundary functions to restrict the realm of action of PREs during the maintenance phase. This activity is most clearly demonstrated by the experiment in which we inverted a fragment within 8XS that contains both the *Fab-8* boundary and the *iab-8* PRE. In its normal orientation, the *iab-8* PRE maintains the β-galactosidase expression pattern initiated by the *iab-8* initiators in PS13, while it is unable to maintain the expression pattern activated by the *iab-7* initiators in PS12. However, when the *iab-8* PRE is placed on the same side of the boundary as the *iab-7* initiators, it maintains the PS12 β-galactosidase expression pattern induced by these elements, but fails to maintain the pattern activated by the *iab-8* initiators. Further evidence that the *Fab-8* boundary restricts the spread of *Pc-G* silencing complexes comes from a comparison of the phenotypes of a deletion that removes just the boundary with a deletion that removes both the boundary and the PRE. Whereas the former exhibits a mixture of gain- and loss-of-function transformations in PS12, the latter exhibits only a gain-of-function transformation of PS12 into PS13.

Organization and functioning of the *Abd-B cis*-regulatory domains

The studies reported here taken together with previous work on *Fab-7* indicate that the *iab-7 cis*-regulatory domain spans a DNA segment of approximately 18 kb. The proximal side of this domain is delimited by the *Fab-7* boundary, while the distal side is marked by the *Fab-8* boundary. Located immediately adjacent to the *Fab-7* boundary, just within the proximal edge of the *iab-7* domain is an *iab-7*PRE. A similar organization of boundary and PRE is seen on the other side of *iab-7*; just beyond the distal edge of the *Fab-8* boundary is an *iab-8*PRE. In addition to this similarity in organization of boundary and PRE, our results suggest that the functional properties of the corresponding elements are remarkably similar. Deletions that remove *Fab-7* fuse the *iab-7 cis*-regulatory domain with *iab-6*, while deletions that remove *Fab-8* fuse *iab-7* with *iab-8*. In both cases, the fused domains misfunction in the specification of parasegment identity, PS11 for *Fab-7* deletions and PS12 for *Fab-8* producing a mixture of gain- and loss-of-function phenotypes in the affected parasegment. This mixed phenotype appears to arise from the ectopic activation of the more distal (posterior) *cis*-regulatory domain (*iab-7* for *Fab-7* and *iab-8* for *Fab-8*) or the ectopic silencing of the more proximal (anterior) *cis*-regulatory domain (*iab-6* for *Fab-7* and *iab-7* for *Fab-8*). Finally deletions that remove both the boundary and the PRE exhibit only the gain-of-function phenotype; in the case of the *Fab-7:iab-7* PRE deletion, a PS11-to-PS12 transformation while in the case of the *Fab-8:iab-8* PRE deletion, a PS12-to-PS13 transformation.

The identification of a second boundary element in the *Abd-B* regulatory region of BX-C, besides suggesting that there may be similar elements elsewhere in the complex, poses the question of how the boundaries block cross-talk between adjacent domains without preventing these domains from interacting with the *Abd-B* promoter. This problem can be illustrated for the *iab-6 cis*-regulatory domain, which controls *Abd-B* in PS11 (see Fig. 1). The *Fab-7* and *Fab-8* boundaries are interposed between *iab-6* and the *Abd-B* gene, and thus might be expected to prevent regulatory interactions between this domain and the *Abd-B* promoter. Moreover, there is ample evidence that both *Fab-7* and *Fab-8* are capable of blocking enhancer:promoter interactions not only in transgenes assays but also in the context of BX-C itself. One good example is the parasegmental expression pattern of the *Bluetail* transposon which is inserted between the *Fab-7* boundary and the *iab-7* PRE. When *Fab-7* is present, it insulates *Bluetail* from regulatory interactions with *iab-6*; however, when the boundary is deleted, *Bluetail* is activated in PS11 (Mihaly et al., 1997). The *fs(3)5649* enhancer trap on the distal side of *iab-7* also appears to be insulated from regulatory interactions with either *iab-6* or *iab-8*.

A number of factors might enable the *Fab-7* and *Fab-8* boundaries to function selectively, insulating the *cis*-regulatory domains from each other, but having little or no effect on their interactions with the *Abd-B* promoter. One factor is the strength of the boundary. The blocking activity of both *Fab-7* (see Hagstrom et al., 1996) and *Fab-8* in transgene assays is clearly not as strong as an intact *su(Hw)* insulator, which contains twelve binding sites for the Su(Hw) protein. A second factor may be the presence of special tethering elements upstream of the *Abd-B* promoter, which are not present in the promoters of the transposons. Recent studies by Sipos et al. (1998) on transvection in the *Abd-B* domain of BX-C have shown that there is an extensive region upstream of the *Abd-B* promoter that mediates long distance interactions with *cis*-regulatory domains. It is possible that these special tethering elements help over come the insulating activities of boundaries like *Fab-7* and *Fab-8*.

We wish to thank David Kuhn for his advice for the larval cuticle preparations and Elvire Martinez for photographs. The authors acknowledge HFSP whose support during the initial phases of the work made the collaborative project possible. S. B., J. M., M. G. and F. K. were supported by grants from the Swiss National Science Foundation and the State of Geneva. M. M. was supported by an EMBO Long Term Fellowship and by an Advanced Fellowship from the Swiss National Science foundation. G. S. was supported by an NIH Post-Doctoral Fellowship. The research of M. M., K. H., G. S. and P. S. was supported by a grant from NIH. H. G. was supported by the Hungarian National Science Foundation (OTKA T 021051).

REFERENCES

Boivin, A. and Dura, J. M. (1998). In vivo chromatin accessibility correlates with gene silencing in Drosophila. *Genetics* **150**, 1539-1549.

Brown, J. L., Mucci, D., Whiteley, M., Dirksen, M. L. and Kassis, J. A. (1998). The Drosophila Polycomb group gene pleiohomeotic encodes a DNA binding protein with homology to the transcription factor YY1. *Mol. Cell* **1**, 1057-1064.

Celniker, S. E., Sharma, S., Keelan, D. J. and Lewis, E. B. (1990). The molecular genetics of the bithorax complex of Drosophila: cis-regulation in the Abdominal-B domain. *EMBO J.* **9**, 4277-4286.

Chan, C. S., Rastelli, L. and Pirrotta, V. (1994). A Polycomb response element in the Ubx gene that determines an epigenetically inherited state of repression. *EMBO J.* **13**, 2553-2564.

Chiang, A., O'Connor, M. B., Paro, R., Simon, J. and Bender, W. (1995). Discrete Polycomb binding sites in each parasegmental domain of the bithorax complex. *Development* **121**, 1681-1689.

Donze D., Adams C. R., Rine J. and Kamakaka, R. T. (1999). The boundaries of the silenced HMR domain in Saccharomyces cerevisiae. *Genes Dev.* **13**, 698-708

Duncan, I. (1987). The bithorax complex. *Annu. Rev. Genet.* **21**, 285-319.

Galloni, M., Gyurkovics, H., Schedl, P. and Karch, F. (1993). The bluetail transposon: evidence for independent cis-regulatory domains and domain boundaries in the bithorax complex. *EMBO J.* **12**, 1087-1097.

Gerasimova, T. I. and Corces, V. G. (1996). Boundary and insulator elements in chromosomes. *Curr. Opin. Genet. Dev.* **6**, 185-192.

Geyer, P. (1997). The role of insulator elements in defining domains of gene expression. *Curr. Opin. Genet. Dev.* **7**, 241-248.

Gloor, G. B., Preston, C. R., Johnson-Schlitz, D. M., Nassif, N. A., Phillis, R. W., Benz, W. K., Robertson, H. M. and Engels, W. R. (1993) Type I repressors of P element mobility. *Genetics* **135**, 81-95.

Gyurkovics, H., Gausz, J., Kummer, J. and Karch, F. (1990). A new homeotic mutation in the Drosophila bithorax complex removes a boundary separating two domains of regulation. *EMBO J.* **9**, 2579-2585.

Hagstrom, K., Muller, M. and Schedl, P. (1996). *Fab-7* functions as a chromatin domain boundary to ensure proper segment specification by the *Drosophila* bithorax complex. *Genes Dev.* **10**, 3202-3215.

Hagstrom, K., Muller, M. and Schedl, P. (1997). A *Polycomb* and GAGA dependent silencer adjoins the *Fab-7* boundary in the *Drosophila* bithorax complex. *Genetics **146***, 1365-1380.

Karch, F., Galloni, M., Sipos, L., Gausz, J., Gyurkovics, H. and Schedl, P. (1994). Mcp and Fab-7: molecular analysis of putative boundaries of cis-regulatory domains in the bithorax complex of *Drosophila melanogaster*. *Nucleic Acids Res.* **22**, 3138-3146.

Kennison, J. A. and Tamkun, J. W. (1992). Trans-regulation of homeotic genes in Drosophila. *New Biol.* **4,** 91-96.

Lewis, E. B. (1978). A gene complex controlling segmentation in *Drosophila*. *Nature* **276,** 565-570.

Martin, C., Mayeda, C., Davis, C., Ericsson, C., Knafels, J., Mathog, D., Celniker, S., Lewis, E. and Palazzolo, M. (1995). Complete sequence of the bithorax complex of *Drosophila*. *Proc. Natn. Acad. Sci., USA* **92**, 8398-8402.

McCall, K. and Bender, W. (1996). Probes of chromatin accessibility in the Drosophila bithorax complex respond differently to Polycomb-mediated repression. *EMBO J.* **15**, 569-580.

Mihaly, J., Hogga, I., Gausz, J., Gyurkovics, H. and Karch, F. (1997). In situ dissection of the Fab-7 region of the bithorax complex into a chromatin domain boundary and a Polycomb-response element. *Development* **124**, 1809-1820.

Mihaly, J., Hogga, I., Barges, S., Galloni, M., Mishra, R. K., Hagstrom, K., Muller, M., Schedl, P., Sipos, L., Gausz, J., Gyurkovics, H. and Karch, F. (1998). Chromatin domain boundaries in the Bithorax complex. *Cell Mol. Life Sci.* **54**, 60-70.

Mihaly, J., Mishra, R. K. and Karch, F. (1998). A conserved sequence motif in Polycomb-response elements. *Mol. Cell* **1**, 1065-1066.

Muller, J. and Bienz, M. (199l). Long range repression conferring boundaries of Ultrabithorax expression in the *Drosophila* embryo. *EMBO J.* **10**, 3147-3155.

Muller, J. and Bienz, M. (1992) Sharp anterior boundary of homeotic gene expression conferred by the *fushi tarazu* protein. *EMBO J.* **11**, 3653-3661.

Paro, R. (1990). Imprinting a determined state into the chromatin of Drosophila. *Trends Genet.* **6,** 416-421.

Peifer, M., Karch, F. and Bender, W. (1987). The bithorax complex: control of segmental identity. *Genes Dev.* **1**, 891-898.

Pirrotta, V. (1997). Chromatin-silencing mechanisms in Drosophila maintain patterns of gene expression. *Trends Genet.* **13**, 314-318.

Poux, S., Kostic, C. and Pirrotta, V. (1996). Hunchback-independent silencing of late *Ubx* enhancers by a Polycomb Group Response Element. *EMBO J.* **15**, 4713-4722.

Qian, S., Capovilla, M. and Pirrotta, V. (1991). The bx region enhancer, a distant cis-control element of the Drosophila Ubx gene and its regulation by hunchback and other segmentation genes. *EMBO J.* **10**, 1415-1425.

Sanchez-Herrero, E., Vernos, I., Marco, R. and Morata, G. (1985). Genetic organization of the *Drosophila* bithorax complex. *Nature* **313**, 108-113.

Sanchez-Herrero, E. (1991). Control of the expression of the bithorax complex genes abdominal-A and abdominal-B by cis-regulatory regions in Drosophila embryos. *Development* **111**, 437-449.

Simon, J., Peifer, M., Bender, W. and O'Connor, M. (1990). Regulatory elements of the bithorax complex that control expression along the anterior-posterior axis. *EMBO J.* **9**, 3945-3956.

Simon, J., Chiang, A., Bender, W., Shimell, M. J. and O'Connor, M. (1993). Elements of the Drosophila bithorax complex that mediate repression by Polycomb group products. *Dev. Biol.* **158**, 131-144.

Simon, J. (1995). Locking in stable states of gene expression: transcriptional control during Drosophila development. *Curr. Opin. Cell Biol.* **7**, 376-385.

Sipos, L., Mihaly, J., Karch, F., Schedl, P., Gausz, J. and Gyurkovics, H. (1998). Transvection in the Drosophila *Abd-B* domain. Extensive upstream sequences are involved in anchoring distant cis-regulatory regions to the promoter. *Genetics* **149,** 1031-1050.

Van der Meer, J. M. (1977). Optical clean and permandent whole mount preparation for phase constrast microscopy of cuticular structures of insect larvae. *Drosophila Inf. Service* **52**, 160.

Zavortink, M. and Sakonju, (1989). The morphogenetic and regulatory functions of the *Drosophila Abdominal-B* gene are encoded in overlapping RNAs transcribed from separate promoters. *Genes Dev.* **3**, 1969-1981.

Zhou, J., Barolo, S., Szymanski, P. and Levine, M. (1996). The Fab-7 element of the bithorax complex attenuates enhancer-promoter interactions in the *Drosophila* embryo. *Genes Dev.* **15** 3195-3201.

Zhou J., Ashe H., Burks C. and Levine, M. (1999). Characterization of the transvection mediating region of the abdominal-B locus in *Drosophila*. *Development* **126**, 3057-3065.